Ultrafast gain dynamics in N_2^+ lasing from highly excited vibrational states pumped by circularly polarized femtosecond laser pulses

Kaixuan Zhai (翟凯旋)[1,2], Ziting Li (李紫婷)[1,2,3], Hongqiang Xie (谢红强)[1,2], Chenrui Jing (井晨睿)[1,2], Guihua Li (李贵花)[1], Bin Zeng (曾 斌)[1], Wei Chu (储 蔚)[1], Jielei Ni (倪洁蕾)[1], Jinping Yao (姚金平)[1,*], and Ya Cheng (程 亚)[1]

[1]*State Key Laboratory of High Field Laser Physics, Shanghai Institute of Optics and Fine Mechanics, Chinese Academy of Sciences, Shanghai 201800, China*

[2]*University of Chinese Academy of Sciences, Beijing 100049, China*

[3]*School of Physics Science and Engineering, Tongji University, Shanghai 200092, China*

**Corresponding author: jinpingmrg@163.com*

Received January 26, 2015; accepted March 16, 2015; posted online April 20, 2015

We experimentally demonstrate N_2^+ lasing actions at the wavelengths of 353.3, 353.8, and 354.9 nm using a circularly polarized femtosecond laser. The three laser lines correspond to the $B^2\Sigma_u^+(v'=5,4,3) \rightarrow X^2\Sigma_g^+(v=4,3,2)$ transitions, respectively. Particularly, we reveal the pressure-dependent gain dynamics of these lasing actions from highly excited vibrational states with a pump–probe scheme. Our experimental results confirm that electron collisional excitation plays an important role in the establishment of a population inversion of N_2^+ lasing at these wavelengths.

OCIS codes: 020.2649, 320.7150, 320.2250.
doi: 10.3788/COL201513.050201.

The interaction of ultrashort laser pulses with matter has been an important research field due to the rich physical phenomena involved in this process, as well as its promising applications[1–9]. In particular, air lasing has recently attracted significant attention as a novel ultrafast nonlinear optical phenomenon. Air lasing enables the generation of highly directional, high-brightness, narrow-bandwidth coherent emissions, and thus provides great potential for enhancing precision and sensitivity in the remote detection and identification of pollutants in the atmosphere. Generally, air lasers can be divided into two categories: amplified spontaneous emission (ASE)[10–16] and seed amplification[17–29]. Air lasers in the former category have been realized in both the forward and backward directions with molecular nitrogen[10–13], atomic oxygen[14,15] or nitrogen[15,16] as the gain media. In particular, the backward air lasers would provide a new strategy to meet the pressing needs of various environmental issues. For the latter category, lasing actions have only been observed in neutral[17–19] and ionic[20–29] nitrogen molecules in the forward direction. In this scheme, upon the injection of a seed pulse, the air laser signal will be enhanced by several orders of magnitude[18,19,21,23,24,29] and will inherit the polarization properties of the seed pulse[18–21,23], which is different from the random polarization of ASE-based lasers[30]. Furthermore, the presence of the seed pulse renders it possible to perform pump–probe measurements. These characteristics make it an ideal tool for the investigation of ultrafast molecular processes in strong laser fields[18,19,21,24,27,28].

At present, the pumping mechanism behind the tunnel ionization-induced nitrogen molecular ion (N_2^+) lasers has not been completely clarified[20,21,31–36]. Most previous investigations on such N_2^+ lasers mainly focus on the two typical laser lines at ~391 and ~428 nm[21–29], which correspond to the $B^2\Sigma_u^+(v'=0) \rightarrow X^2\Sigma_g^+(v=0,1)$ transitions, respectively. Typically, the two laser lines were excited with linearly polarized pump pulses because it was found that excitation with linearly polarized laser fields could be more efficient than with circularly polarized ones[29]. This finding could be understood in the framework of strong field ionization[37], in which ionization with linearly polarized light is more efficient because of its higher electric field strength than that of circularly polarized light.

Surprisingly, our recent experiment shows that some N_2^+ laser lines from the highly excited vibrational states of the $B^2\Sigma_u^+$ and $X^2\Sigma_g^+$ states (i.e., 353.3, 353.8, and 354.9 nm) can only be efficiently generated with circularly polarized laser pulses[38]. This observation indicates that impact excitation by the hot electrons generated in the femtosecond laser fields could play a critical role in the generation of these laser lines. In this work, to clarify the pumping mechanism, we perform pump–probe measurements with an external seed pulse, the spectrum of which covers the wavelengths of the three laser lines from the highly excited vibrational states. The ultrafast gain dynamics of these three laser lines provide important information for determining their origin, and reveal the rich physics involved in various types of N_2^+ lasers that are produced by femtosecond pump lasers.

In the experiment, the femtosecond laser pulses (~40 fs, 800 nm, ~12.8 mJ, 1 kHz) from a commercial Ti:sapphire laser (Legend Elite Cryo PA, Coherent, Inc.) were split

into two beams with a 4:1 beam splitter. One beam with the pulse energy of ~10 mJ was transformed into circularly polarized light through a quarter-wave plate, and then served as the pump to build up the population inversion between the highly excited vibrational states of the $B^2\Sigma_u^+$ and $X^2\Sigma_g^+$ states. The other beam was used to generate the wavelength-tunable, linearly polarized seed pulse (i.e., the probe pulse). Similar to our previous work[18], the seed pulse was generated by the method discussed below. The second laser beam was firstly directed into a 20 mm-long BK7 glass to generate the supercontinuum white light, and then the supercontinuum was frequency doubled in a 2 mm-thick β-BaB_2O_4 (BBO) crystal. By adjusting the phase-matched angle of the BBO crystal to select the spectral component of the supercontinuum light to be frequency doubled efficiently, we can continuously tune the central wavelength of the seed pulse. The pump and seed pulses were collinearly combined using a dichroic mirror with a high reflectivity around 800 nm and a high transmission in the 290–660 nm spectral range. They were then focused by an $f = 30$ cm plano-convex lens into the gas chamber filled with high-purity nitrogen gas. The time delay between the pump and the probe was controlled by a motorized linear translation stage, which was placed in the probe beam. The output signal was collimated by an $f = 30$ cm lens into a grating spectrometer (Shamrock 303i, Andor) after the residual 800 nm pump pulses were removed through filters.

Figures 1(a)–1(c) show the pressure-dependent forward spectra recorded with the circularly polarized pump pulses when the central wavelength of the seed pulses is fixed at 355.4 nm. The time delay between the pump and the probe pulses is optimized to obtain strong laser signals at the three gas pressures used in the experiment. In Fig. 1(a), it can be clearly seen that at the gas pressure of 22 mbar, three narrow-bandwidth spectral peaks at the wavelengths of 353.3, 353.8, and 354.9 nm

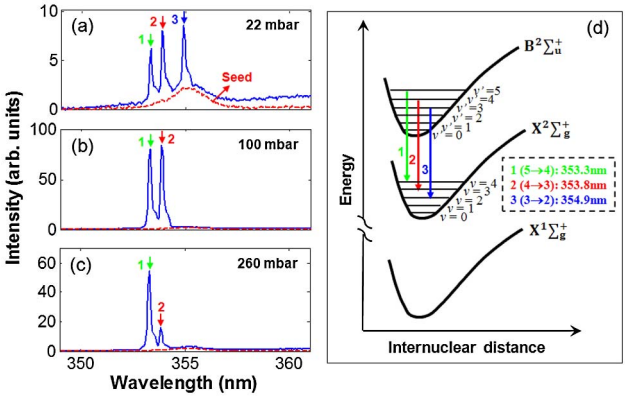

Fig. 1. Forward spectra recorded at the gas pressures of (a) 22, (b) 100, and (c) 260 mbar in a pump–probe scheme. (d) Energy level diagram of the ionized and neutral nitrogen molecules in which the $B^2\Sigma_u^+(v' = 5, 4, 3) \rightarrow X^2\Sigma_g^+(v = 4, 3, 2)$ transitions are indicated with the corresponding lasing wavelengths.

simultaneously appear on top of the seed spectrum, which correspond to the $B^2\Sigma_u^+(v' = 5, 4, 3) \rightarrow X^2\Sigma_g^+(v = 4, 3, 2)$ transitions, respectively, as indicated in Fig. 1(d)[39]. Under this condition, the intensities of these three spectral lines are comparable, and their gain factors are measured to be ~13, ~8, and ~4, respectively. Here, the gain factor is defined as the ratio between the intensities of the laser signals and those of the seed pulses at the lasing wavelengths of 353.3, 353.8, and 354.9 nm. Additionally, once the seed pulse is removed, the three laser lines will disappear, i.e., the laser lines will drop to the level of the background. This observation provides strong evidence on the establishment of a population inversion between the highly excited vibrational energy levels of the $B^2\Sigma_u^+$ and $X^2\Sigma_g^+$ states, as well as the existence of the seeding effect. When the gas pressure increases to 100 mbar, the laser signals at the wavelengths of 353.3 and 353.8 nm will be significantly enhanced, whereas the laser signal at 354.9 nm becomes hardly detectable, as illustrated in Fig. 1(b). In this case, the gain factors of the 353.3 and 353.8 nm laser signals are up to ~174 and ~88, respectively. When the gas pressure further increases to 260 mbar, the two laser signals at 353.3 and 353.8 nm will decrease, as shown in Fig. 1(c).

It is also noteworthy that similar to our previous observation[38], the three spectral lines can only be efficiently generated in a small range around the circular polarization. This fact suggests that collisional excitation by the high-energy electrons should play the key role in the establishment of the population inversion, since the tunnel-ionized electrons can gain higher energy from circularly polarized laser field than from linearly polarized one[40]. Based on the electron impact excitation mechanism, we can qualitatively explain the dependence of these laser signals on the gas pressure. On the one hand, the effective electron collisional excitation requires high-density gaseous molecules and electrons, which means that high gas pressures are beneficial for achieving lasing. On the other hand, at high gas pressures, the collision between molecular ions at the excited states and neutral molecules at the ground states (i.e., collisional quenching) will become efficient, too. This process can depopulate the excited molecular ions. The compromise between these two processes leads to the optimized pressure, as shown in Fig. 1. We also notice that the laser signal at 354.9 nm can only be observed at a relatively low gas pressure, which is significantly different from the two other laser signals (i.e., 353.3 and 353.8 nm). It could be due to the different rates of both the collisional excitation and the collisional quenching for different vibrational transitions.

To provide further evidence on the seeding effect, we also investigate the intensities of these three laser lines from highly excited vibrational states as functions of the central wavelength of the seed pulses at an optimized time delay and at a gas pressure of 22 mbar. Here, the seed wavelength is scanned from 350.2 to 359.2 nm by tuning the phase-matched angle of the BBO crystal. From Fig. 2, we can clearly see that when the central wavelength of the

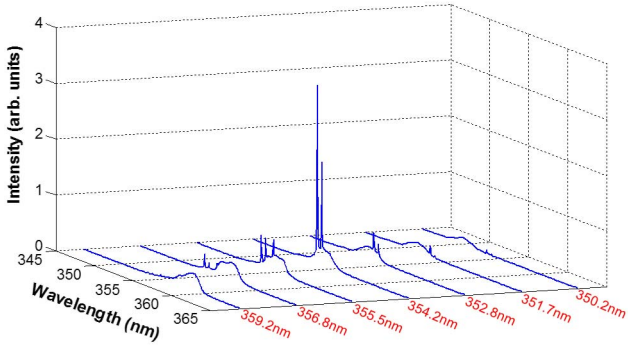

Fig. 2. Forward spectra captured at the different wavelengths of the seed pulses. The central wavelengths of the seed pulses are indicated on the side of the corresponding spectra.

seed pulses is 354.2 nm, both laser signals at 353.3 and 353.8 nm are the strongest, whereas the laser signal at 354.9 nm reaches its maximum at the seed wavelength of 355.5 nm. Once the central wavelength of the seed pulses is tuned away from the wavelengths of the three laser lines, their intensities will rapidly decrease. The high sensitivity of the laser emission on the seed wavelength offers another piece of evidence for the seed amplification mechanism for the lasing actions observed in this experiment.

Furthermore, in order to obtain the ultrafast dynamics of population inversion established between the highly excited vibrational states of the $B^2\Sigma_u^+$ and $X^2\Sigma_g^+$ states, we measured the 353.3, 353.8, and 354.9 nm laser signals as functions of the time delay between the pump and probe pulses at the gas pressures of 22, 100, and 260 mbar. As shown in Fig. 1, these three spectral lines can only be observed simultaneously at the gas pressure of 22 mbar. Therefore, we firstly compare the gain dynamics of these three laser lines at this gas pressure. As shown in Figs. 3(a)–3(c), the laser signals from the different highly excited vibrational states show almost the same tendency with the increase of the time delay between the pump and the probe pulses. All of them first increase rapidly on the time scale of hundreds of femtoseconds, and then show a slow exponential decay. From these curves, the gain lifetime (FWHM) of the three laser lines is estimated to be ~2 ps. When the gas pressure is increased to above 100 mbar, only two laser lines at 353.3 and 353.8 nm can be observed. Therefore, we investigate the gain dynamics of these two laser signals at three different gas pressures. In Fig. 4, we can clearly see that for both the 353.3 and 353.8 nm laser signals, the gain lifetime becomes short with the increase in the gas pressure, which is due to the fact that the stronger collisions among molecules at higher gas pressure results in the decay of the inverted population density. However, at all the three gas pressures, it takes the same amount of time for the population inversion to reach the maximum value.

Based on the above experimental results, we would like to give some quantitative analyses on the mechanism of population inversion. Our previous investigation[38]

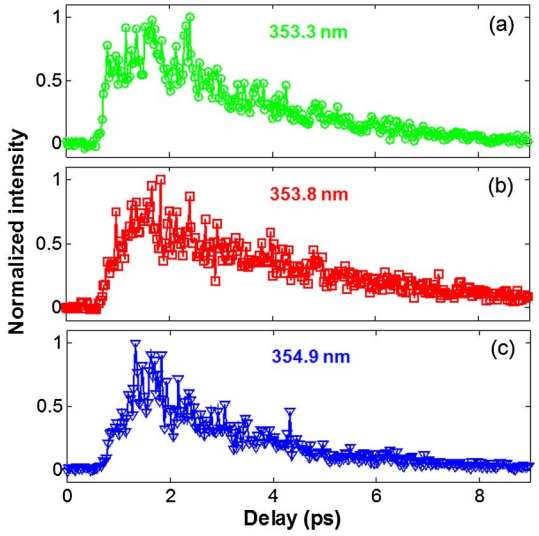

Fig. 3. The temporal evolution of the N_2^+ laser at the wavelengths of (a) 353.3, (b) 353.8, and (c) 354.9 nm with the time delay between the pump and probe pulses at a gas pressure of 22 mbar.

suggested that the population inversion between the $B^2\Sigma_u^+(v' = 3, 4, 5)$ and the $X^2\Sigma_g^+(v = 2, 3, 4)$ states is likely established by the two steps given below. Firstly, the neutral nitrogen molecules are ionized by the laser field. Most of the ions are populated at the low vibrational energy levels of the $X^2\Sigma_g^+$ state (e.g., $v = 0, 1$) which is determined by the Franck–Condon factors[41]. Afterwards, the ground-state ions can be excited to the high vibrational energy

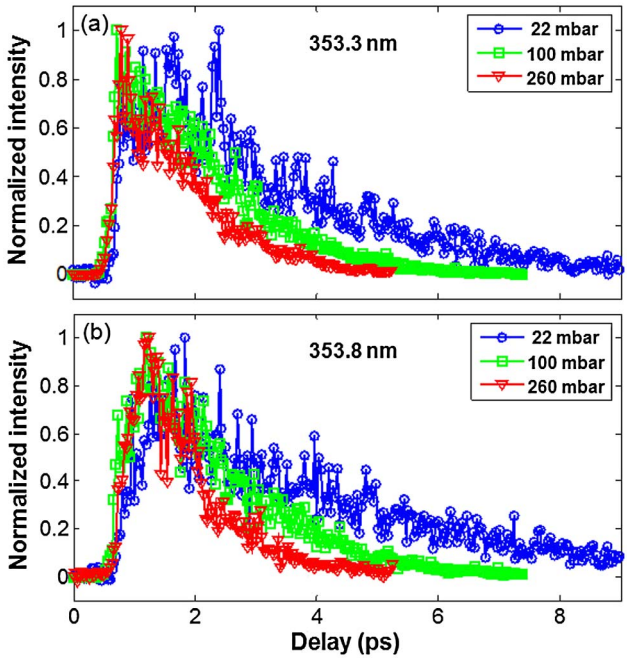

Fig. 4. The temporal evolution of the N_2^+ laser at the wavelengths of (a) 353.3 and (b) 353.8 nm with the time delay between the pump and probe pulses at gas pressures of 22, 100, and 260 mbar.

levels of the $B^2\Sigma_u^+$ state through the collision process between electrons and ions, namely, $N_2^+(X^2\Sigma_g^+, v = 0, 1) + e \rightarrow N_2^+(B^2\Sigma_u^+, v' = 3, 4, 5) + e$. As shown in Ref. [42], the threshold of electron collisional excitation for this collisional reaction is ~4 eV. The collisional excitation cross section will decrease rapidly below the threshold, whereas the cross section will decrease slowly above the threshold. Furthermore, according to the Franck–Condon principle, only a small amount of ions are populated at the lower energy levels to generate laser emission at 353.3, 353.8, and 354.9 nm, i.e., $X^2\Sigma_g^+(v = 4, 3, 2)$[41]. Therefore, population inversion can be built up between the highly excited vibrational energy levels of the $B^2\Sigma_u^+$ and $X^2\Sigma_g^+$ states if the electron energy is higher than 4 eV. Under our experimental conditions (i.e., 10 mJ, 800 nm, ~40 fs), the peak power is estimated as 250 GW, which is above the critical power of self-focusing in the 100 mbar nitrogen gas (i.e., ~42 GW)[4]. Therefore, filamentation will occur at this gas pressure. This means that the laser intensity in the sample will be clamped at $\sim 1 \times 10^{14}$ W/cm^2[43]. At the pump intensity, the electron will obtain an average kinetic energy of ~12 eV from the circularly polarized laser field[40]. For this electron energy, the collisional excitation cross section is about 10^{-16} cm^2[42]. Therefore, population inversion can be easily established between the $B^2\Sigma_u^+(v' = 3, 4, 5)$ and $X^2\Sigma_g^+(v = 2, 3, 4)$ states through strong field ionization followed by the electron collisional excitation in the circularly polarized laser field.

In conclusion, we demonstrate the seed-amplified laser actions at 353.3, 353.8, and 354.9 nm, which correspond to the $B^2\Sigma_u^+(v' = 5, 4, 3) \rightarrow X^2\Sigma_g^+(v = 4, 3, 2)$ transitions, respectively. We systematically investigate the dependence of these three laser lines on gas pressure and seed wavelength. Furthermore, we obtain the information on the gain dynamics by measuring these laser signals as functions of the pump–probe delay. It is found that the lifetime of population inversion critically depends on the gas pressure. Based on these experimental observations, we suggest that strong field ionization followed by electron impact excitation is likely the major pumping mechanism for the transitions between the highly excited vibrational energy levels of the $B^2\Sigma_u^+$ and $X^2\Sigma_g^+$ states.

This work was supported by the National Basic Research Program of China (Grant Nos. 2011CB808102 and 2014CB921300), the National Natural Science Foundation of China (Grant Nos. 11134010, 11204332, and 11304330) and the Program of Shanghai Subject Chief Scientist (Grant No. 11XD1405500).

References

1. T. Popmintchev, M. Chen, D. Popmintchev, P. Arpin, S. Brown, S. Ališauskas, G. Andriukaitis, T. Balčiunas, O. D. Mücke, A. Pugzlys, A. Baltuška, B. Shim, S. E. Schrauth, A. Gaeta, C. Hernández-García, L. Plaja, A. Becker, A. Jaron-Becker, M. M. Murnane, and H. C. Kapteyn, Science **336**, 1287 (2012).
2. F. Krausz and M. Ivanov, Rev. Mod. Phys. **81**, 163 (2009).
3. W. Becker, F. Grasbon, R. Kopold, D. B. Milošević, G. G. Paulus, and H. Walther, Adv. At. Mol. Opt. Phys. **48**, 35 (2002).
4. A. Couairon and A. Mysyrowicz, Phys. Rep. **441**, 47 (2007).
5. T. Wang, S. Yuan, Y. Chen, and S. L. Chin, Chin. Opt. Lett. **11**, 011401 (2013).
6. J. Yao, G. Li, X. Jia, X. Hao, B. Zeng, C. Jing, W. Chu, J. Ni, H. Zhang, H. Xie, C. Zhang, Z. Zhao, J. Chen, X. Liu, Y. Cheng, and Z. Xu, Phys. Rev. Lett. **111**, 133001 (2013).
7. H. Xu, A. Azarm, and S. L. Chin, Chin. Opt. Lett. **12**, 113201 (2014).
8. M. Rodriguez, R. Sauerbrey, H. Wille, L. Wöste, T. Fujii, Y.-B. André, A. Mysyrowicz, L. Klingbeil, K. Rethmeier, W. Kalkner, J. Kasparian, E. Salmon, J. Yu, and J.-P. Wolf, Opt. Lett. **27**, 772 (2002).
9. J. Kasparian, M. Rodriguez, G. Méjean, J. Yu, E. Salmon, H. Wille, R. Bourayou, S. Frey, Y.-B. André, A. Mysyrowicz, R. Sauerbrey, J.-P. Wolf, and L. Wöste, Science **301**, 61 (2003).
10. Q. Luo, W. Liu, and S. L. Chin, Appl. Phys. B **76**, 337 (2003).
11. S. Mitryukovskiy, Y. Liu, P. Ding, A. Houard, and A. Mysyrowicz, Opt. Express **22**, 12750 (2014).
12. D. Kartashov, S. Ališauskas, G. Andiukaitis, A. Pugžlys, M. Shneider, A. Zheltikov, S. L. Chin, and A. Baltuška, Phys. Rev. A **86**, 033831 (2012).
13. T. Zeng, J. Y. Zhao, W. Liu, and S. L. Chin, Laser Phys. Lett. **11**, 075401 (2014).
14. A. Dogariu, J. B. Michael, M. O. Scully, and R. B. Miles, Science **331**, 442 (2011).
15. A. Laurain, M. Scheller, and P. Polynkin, Phys. Rev. Lett. **113**, 253901 (2014).
16. A. Dogariu and R. B. Miles, in *CLEO: 2013* (Optical Society of America, 2013), paper QW1E.1.
17. D. Kartashov, S. Ališauskas, A. Baltuška, A. Schmitt-Sody, W. Roach, and P. Polynkin, Phys. Rev. A **88**, 041805(R) (2013).
18. J. Yao, Q. Xie, B. Zeng, W. Chu, G. Li, J. Ni, H. Zhang, C. Jing, C. Zhang, H. Xu, Y. Cheng, and Z. Xu, Opt. Express **22**, 19005 (2014).
19. P. Ding, S. Mitryukovskiy, A. Houard, E. Oliva, A. Couairon, A. Mysyrowicz, and Y. Liu, Opt. Express **22**, 29964 (2014).
20. J. Yao, B. Zeng, H. Xu, G. Li, W. Chu, J. Ni, H. Zhang, S. L. Chin, Y. Cheng, and Z. Xu, Phys. Rev. A **84**, 051802(R) (2011).
21. J. Yao, G. Li, C. Jing, B. Zeng, W. Chu, J. Ni, H. Zhang, H. Xie, C. Zhang, H. Li, H. Xu, S. L. Chin, Y. Cheng, and Z. Xu, New J. Phys. **15**, 023046 (2013).
22. Y. Liu, Y. Brelet, G. Point, A. Houard, and A. Mysyrowicz, Opt. Express **21**, 22791 (2013).
23. T. Wang, J. F. Daigle, J. Ju, S. Yuan, R. Li, and S. L. Chin, Phys. Rev. A **88**, 053429 (2013).
24. H. Zhang, C. Jing, J. Yao, G. Li, B. Zeng, W. Chu, J. Ni, H. Xie, H. Xu, S. L. Chin, K. Yamanouchi, Y. Cheng, and Z. Xu, Phys. Rev. X **3**, 041009 (2013).
25. D. Kartashov, J. Möhring, G. Andriukaitis, A. Pugžlys, A. Zheltikov, M. Motzkus, and A. Baltuška, in *Conference on Lasers and Electro-Optics 2012* (Optical Society of America, 2012), paper QTh4E.6.
26. G. Point, Y. Liu, Y. Brelet, S. Mitryukovskiy, P. Ding, A. Houard, and A. Mysyrowicz, Opt. Lett. **39**, 1725 (2014).
27. J. Ni, W. Chu, H. Zhang, B. Zeng, J. Yao, L. Qiao, G. Li, C. Jing, H. Xie, H. Xu, Y. Cheng, and Z. Xu, Opt. Lett. **39**, 2250 (2014).
28. B. Zeng, W. Chu, G. Li, J. Yao, H. Zhang, J. Ni, C. Jing, H. Xie, and Y. Cheng, Phys. Rev. A **89**, 042508 (2014).
29. H. Zhang, C. Jing, G. Li, H. Xie, J. Yao, B. Zeng, W. Chu, J. Ni, H. Xu, and Y. Cheng, Phys. Rev. A **88**, 063417 (2013).
30. S. Yuan, T. Wang, Y. Teranishi, A. Sridharan, S. H. Lin, H. Zeng, and S. L. Chin, Appl. Phys. Lett. **102**, 224102 (2013).
31. S. L. Chin, H. Xu, Y. Cheng, Z. Xu, and K. Yamanouchi, Chin. Opt. Lett. **11**, 013201 (2013).

32. G. Andriukaitis, J. Möhring, D. Kartashov, A. Pugžlys, A. Zheltikov, M. Motzkus, and A. Baltuška, in *EPJ Web of Conferences* (2013), Vol. **41**, p. 10004.
33. J. Ni, W. Chu, C. Jing, H. Zhang, B. Zeng, J. Yao, G. Li, H. Xie, C. Zhang, H. Xu, S. L. Chin, Y. Cheng, and Z. Xu, Opt. Express **21**, 8746 (2013).
34. G. Li, C. Jing, B. Zeng, H. Xie, J. Yao, W. Chu, J. Ni, H. Zhang, H. Xu, Y. Cheng, and Z. Xu, Phys. Rev. A **89**, 033833 (2014).
35. A. Baltuška and D. Kartashov, in *Research in Optical Sciences* (Optical Society of America, 2014), paper HTh4B.5.
36. P. Wang, S. Xu, D. Li, H. Yang, H. Jiang, Q. Gong, and C. Wu, Phys. Rev. A **90**, 033407 (2014).
37. A. Talebpour, M. Abdel-Fattah, A. D. Bandrauk, and S. L. Chin, Laser Phys. **11**, 68 (2001).
38. C. Jing, J. Yao, Z. Li, J. Ni, B. Zeng, W. Chu, G. Li, H. Xie, and Y. Cheng, J. Phys. B At. Mol. Opt. Phys. **48**, 094001 (2015).
39. R. W. B. Pearse and A. G. Gaydon, *The Identification of Molecular Spectra* (John Wiley & Sons, New York, 1976).
40. P. B. Corkum, Phys. Rev. Lett. **71**, 1994 (1993).
41. F. R. Gilmore, R. R. Laher, and P. J. Espy, J. Phys. Chem. Ref. Data **21**, 1005 (1992).
42. O. Nagy, C. P. Ballance, K. A. Berrington, P. G. Burke, and B. M. McLaughlin, J. Phys. B **32**, L469 (1999).
43. A. Becker, N. Aközbek, K. Vijayalakshmi, E. Oral, C. M. Bowden, and S. L. Chin, Appl. Phys. B **73**, 287 (2001).